Flexible metal-free counter electrode for dye solar cells based on conductive polymer and carbon nanotubes

Kerttu Aitola[a,1,*], Maryam Borghei[a], Antti Kaskela[a], Erno Kemppainen[a], Albert G. Nasibulin[a], Esko I. Kauppinen[a], Peter D. Lund[a], Virginia Ruiz[a,b,2,*], Janne Halme[a,3,*]

[a] *Department of Applied Physics, Aalto University School of Science, P.O. Box 15100, 00076 Aalto, Finland*
[b] *CIDETEC-IK4 - Centre for Electrochemical Technologies, Paseo Miramón 196, E-20009 Donostia-San Sebastián, Spain*

Abstract

The counter electrodes (CE) for flexible dye solar cells (DSC) are normally prepared by sputtering platinum on indium tin oxide (ITO) plastic substrate. However both ITO and platinum are expensive materials that need to be replaced with cheaper alternatives in large scale production of low-cost DSCs. We fabricated a flexible and completely carbon-based CE for DSCs based on electropolymerized poly(3,4-ethylenedioxythiophene) (PEDOT) on single-walled carbon nanotube (SWCNT) film on a plain plastic substrate. The DSCs with such a CE had an efficiency of 4 %, which is similar to the efficiency of the reference DSCs (3.9 %) based on conventional sputtered platinum on ITO-plastic CE. The carbon-based electrode was prepared by a simple press-transfer method of SWCNTs from the collection filter used in the gas phase synthesis and by electrochemical deposition of PEDOT on it. Electrochemical impedance spectroscopy confirmed that the PEDOT-SWCNT film had the best catalytic performance among the studied CE materials, and the film was also slightly transparent. The results demonstrate a succesful combination of the conductive and catalytic properties of SWCNTs and PEDOT, respectively.

1. Introduction

The dye solar cell [1] is one of the possible options for large-scale roll-to-roll production of photovoltaic cells on flexible plastic and metal substrates. The conventional choice for a plastic DSC counter electrode has been sputtered platinum on indium tin oxide-polyethylene terephtalate (ITO-PET) or ITO-polyethylene naphtalate substrates. Sputtering has been the method of

*Corresponding author
[1]Email: kerttu.aitola@aalto.fi
[2]Email: virginia.ruiz@aalto.fi
[3]Email: janne.halme@aalto.fi

Pt deposition, since plastic substrates do not withstand the high temperatures of thermal Pt deposition used with glass substrates. However, Pt and In are expensive and rare metals, and ITO is subjected to cracking when bent [2].

One candidate for the conductive, catalytic and flexible DSC CE material is the randomly oriented single-walled carbon nanotube network [3, 4, 5]. The SWCNT network films are highly flexible [6] and can be deposited on a desired substrate by a simple press-transfer method [7]. When such a film is applied as a DSC CE, the SWCNTs may simultaneously carry out the conductive and the catalytic functions of the CE. However, this type of CE, which, from the point-of-view of manufacturing and flexibility, is preferentially applied as a thin, semi-transparent layer, is as such only moderately catalytically active toward the tri-iodide reduction reaction of the DSC CE [5].

Conductive polymers, such as poly-(3,4-ethylenedioxythiophene) (PEDOT), its poly(styrenesulfonate) (PSS) and *p*-toluenesulfonate doped version, and polyaniline, are promising organic DSC catalysts. These materials have been successfully applied as the DSC CE on glass [8, 9, 10] and plastic [11] substrates, but always in parallel with the conventional transparent conductive layers (ITO or fluorine-doped tin oxide, FTO). PEDOT-carbon nanotube [12, 13, 14], PEDOT:-PSS-carbon black [15] and PEDOT-graphene [16] composites have also been used on FTO or ITO glass. Only in one study, a PEDOT:PSS film on a polyester substrate was studied as the sole CE structure, but the DSCs had a modest 0.05 % efficiency [17].

In this work, we combine the best properties of electrochemically deposited PEDOT and the aforementioned random network SWCNT films and demonstrate a composite counter electrode for flexible DSCs without additional conductive or catalytic layers. The catalytic performance of the resulting PEDOT-SWCNT CE was found superior to the sputtered platinum on ITO-PET and thermally deposited platinum on FTO glass. The catalytic activities of the films were studied with cyclic voltammetry (CV) in an electrochemical 3-electrode cell and with electrochemical impedance spectroscopy (EIS) in the DSC, and the conductivities and optical properties were addressed.

The method of choice for coating the SWCNTs with PEDOT was oxidative electropolymerization of EDOT. This method offers several advantages over other approaches, such as spin-coating: it enables precise control of the amount (thickness) of the polymer, it is fast (in the tens of seconds scale), yet very reproducible, it can be upscaled to large electrode areas and it is carried out at room temperature. In electrodeposition, the underlying SWCNT network provides a conducting, porous platform on which the PEDOT nucleation and coating occurs, maximizing the PEDOT-SWCNT film interfacial area. Thus, the SWCNT network acts as a template during the electropolymerization, leading to porous, wire-like nanostructures with PEDOT wrapping the SWCNT bundles [18].

In this paper, we show that the performance of SWCNT network electrodes on PET plastic as the DSC CE can be significantly improved by electrodepositing PEDOT on them. The result demonstrates a Pt and In free CE alternative for flexible DSCs with performance comparable to sputtered Pt on ITO-PET.

2. Experimental

The SWCNTs used in this study were synthesized by an aerosol CVD process [19], described in detail in the Supporting Information. The SWCNTs are grown and subsequently form small diameter bundles in the gas phase, and the bundles are collected downstream at the outlet of the synthesis reactor by membrane filtration, and the thus formed SWCNT network can be transferred to several substrate materials by a simple room temperature press-transfer process [7]. Here the SWCNT networks were transferred to PET plastic substrates (Goodfellow, Bi-Axially oriented PET) after the SWCNT network was mechanically cut down to the DSC CE dimensions. The SWCNT networks were ethanol densified after the transfer to improve adhesion of the network to the substrate [7, 20].

The SWCNT films were electrochemically purified of iron catalyst particles present in the films from the SWCNT synthesis by anodic stripping in 1 M HNO_3 in an aqueous solution [21] prior to the PEDOT deposition, since iron is known to be detrimental for the DSC photoelectrode (PE) [5]. The method is known to be effective for iron removal from the SWCNT films and non-harmful to the film quality [21]. Electropolymerization of 3,4-ethylenedioxythiophene (EDOT) was conducted on the iron-purified SWCNT films by chronocoulometry, at +1.0 V, in an aqueous solution of 3 mM EDOT and 0.3 M $LiClO_4$. PEDOT films of different thickness were produced by varying the deposition time until reaching different final deposition charge values, ranging from around 7 to 70 s and from 10 - 100 mC/cm^2, respectively.

In order to select the optimal PEDOT-SWCNT CE, the electrocatalytic activity of the films with different PEDOT thicknesses (indicated by the total electrodeposition charge) was evaluated by cyclic voltammetry (CV) in an acetonitrile solution containing 1 mM I_2, 10 mM LiI and 0.1 M $LiClO_4$. It was observed, that thorough rinsing and conditioning of the PEDOT-SWCNT CEs is required for enhanced DSC performance and stability. We also carried out potential cycling of the films in the electrolyte solution to promote releasing of occluded monomers (EDOT) and oligomers from the PEDOT-SWCNT network (see Supporting Information). To ensure further removal of unbound monomer and polymer, the PEDOT-SWCNT films were rinsed with acetonitrile and deionised water and dried with nitrogen flow. Furthermore, prior to the DSC assembly, the PEDOT-SWCNT CEs were conditioned by soaking them overnight in the same electrolyte solution as used in the DSC, and finally rinsed with ethanol and dried.

The solar cells were prepared with the photoelectrode on FTO glass substrate and varying CEs: SWCNT film on PET, PEDOT-SWCNT on PET, sputtered Pt on ITO-PET and thermally deposited Pt on FTO glass (see Supporting Information). The PEs were manufactured by doctor-blading titania paste (Dyesol DSL 18NR-T, average particle diameter 20 nm) on FTO-coated glass with a sheet resistance of 15 Ω/sq (TEC 15, Pilkington, Hartford Glass Company, Inc.) and sintering in air in 450 °C for 30 minutes, to reach TiO_2 films of around 15 μm thickness and 5 mm $\times$ 8 mm geometric area. The PEs were dyed in N719

dye (Dyesol) in ethanol bath for about 17 hours.

The counter electrodes (apart from the thermally platinized FTO glass CEs) were characterized by a multimodal approach, including electrical sheet resistance measurements, optical absorption spectroscopy, field emission SEM and energy dispersive X-ray spectroscopy (EDX). The photovoltaic characterization of the solar cells was carried out in a solar simulator providing a 1 Sun equivalent light intensity. The EIS measurement was carried out in the frequency range 100 kHz - 100 mHz, using 10 mV amplitude, starting from the high-frequency end and sweeping to the low frequencies and back. The measurement was taken in the dark and by polarizing the cells in the voltage range 0 – -0.9V for all the other cells except the SWCNT cells, for which the voltages were 0 – -1.1 V, to obtain similar cell current densities. (All measurement details are listed in the Supporting Information.)

3. Results and Discussion

The effects of the electrochemical cleaning of the iron catalyst particles from the SWCNT networks and the PEDOT deposition were first analyzed by sheet resistance measurements and UV-VIS spectroscopy, summarized in Table 1 and Fig. 1 a). The pristine (ethanol densified) SWCNT networks exhibit a sheet resistance of 13.6 Ω/sq. The SWCNT characteristic optical transitions are clearly visible in Fig. 1 a), indicating high quality SWCNTs. The sheet resistance of the SWCNT film decreases slightly during the electrochemical (EC) cleaning process and the optical transmittance increases somewhat, the latter most likely due to the fact that iron nanoparticles are removed from the film. The semiconducting SWCNT-related optical transitions are suppressed in the EC cleaned samples, likely due to the HNO_3 environment during the cleaning process, which can lead to a partial doping of the SWCNTs and thus explain the reduced sheet resistance of the sample. The electrodeposition of PEDOT on the EC cleaned SWCNT network reduces the transmittance of the film significantly in the visible region, but even more pronouncedly in the IR region of the optical spectrum, while the sheet resistance of the film falls between that of the pristine and the EC cleaned SWCNT networks. However, the stable sheet resistance indicates that the SWCNT network provides the main component to the electrical conduction of the network, while the PEDOT contribution for the improved cell performance is mainly due to the improved catalytic activity discussed later in the paper. Scanning electron microscopy (SEM) confirms that the structural integrity of the SWCNT networks is maintained during the electrochemical cleaning and the PEDOT deposition, see Fig. 1 b) and Supporting Information.

Fig. 2 shows cyclic voltammograms for the SWCNT, PEDOT-SWCNT, bare ITO and PEDOT on ITO electrodes (the latter not studied here in the DSC). The CVs for the PEDOT-SWCNT films exhibit two distinct pairs of redox peaks, I_{ox} and I_{red}, attributed to the oxidation and reduction of I_3^-/I^-, and II_{ox} and II_{red} to the oxidation and reduction of I_2/I_3^- [22]. The PEDOT-SWCNT CV contrasts with the poorer catalytic activity shown by the bare SWCNT

Table 1: Electro-optical properties of the various counter electrode materials studied. EC refers to "electrochemically" and T is optical transmittance.

CE type	R_{SH} (Ω/sq)	T at 550 nm (%)
Ethanol densified SWCNT network	13.6 ± 0.4	9 ± 1
EC cleaned SWCNT network	11.8 ± 0.4	10 ± 1
EC cleaned SWCNT with 33.7 mC/cm^2 PEDOT	12.2 ± 0.4	5 ± 1
ITO-PET	54 ± 2	89 ± 1
ITO-PET-Pt	23 ± 0.7	21 ± 1

electrode, which exhibits much larger peak spacing for the I_3^-/I^- redox couple (the peak spacing is inversely proportional to the rate constant of the electrochemical reaction). The higher current densities together with the smaller peak spacing for the I_3^-/I^- redox reaction obtained for the PEDOT-coated SWCNT electrodes compared to the uncoated SWCNTs are indicative of an expected enhanced performance as DSC CE. However, neither current density nor peak spacing is further improved by increasing the amount of deposited PEDOT beyond 30 mC/cm^2 (see Supporting Information).

The synergistic effect of the separate catalytic activities of PEDOT and SWCNTs is illustrated by comparing the CVs obtained for PEDOT-ITO and PEDOT-SWCNT (and for plain ITO). In the CV of the plain ITO electrode, the redox peaks are missing. For PEDOT-ITO, the two redox peak pairs are broader, located at larger overpotentials and are less reversible than for PEDOT-SWCNT, revealing that the intrinsic catalytic properties of PEDOT alone are not responsible for the improved response. This highlights the collaborative catalytic effect of the SWCNTs and PEDOT, meaning that the SWCNT electrode is a better substrate for the PEDOT catalyst than ITO. This is expected due to the porous structure and the high surface area of the SWCNT network.

The current-voltage (IV) curves of all the studied DSC types are shown in Fig. 3 and the IV parameters in Table 2. The efficiencies of the PEDOT-SWCNT DSCs are 4.0 %, compared to the 2.0 % of the SWCNT-DSCs and similar to those of the sputtered Pt-ITO-PET and thermal Pt-FTO glass DSCs. The good catalytic performance of the PEDOT-SWCNT films is manifested in the good fill factor of the IV curves. For some reason the i_{SC} values are slightly lower for the PEDOT-SWCNT cells than for the other cells, the reason of which we discuss in the following sections.

Example EIS spectra for all the cell types at -0.8 V polarization are shown in Fig. 4 a) (Nyquist plot) and b) (Bode plot). The spectrum of the cells with a plain SWCNT CE is displayed only partially because of its much larger counter electrode charge-transfer resistance, R_{CE}, value at this voltage. The spectra seem typical for all the other cell types, except for the PEDOT-SWCNT cells, where the PE and CE semicircles overlap more than usually. This is because

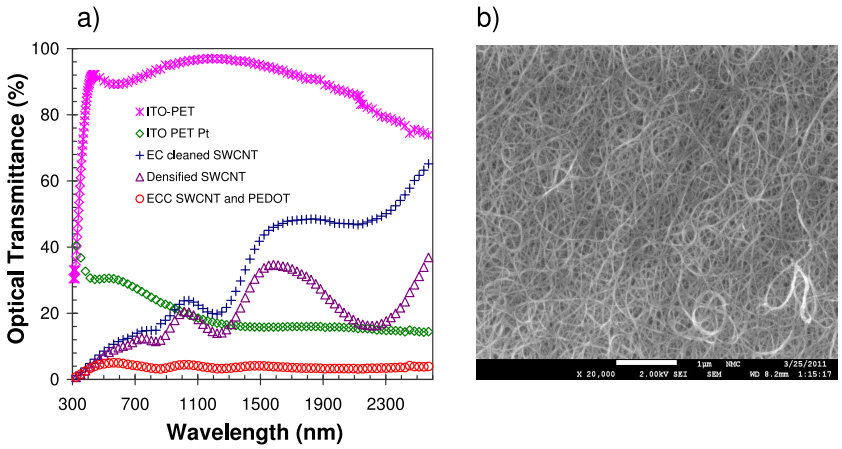

Figure 1: a) Optical transmittance of the SWCNT-based counter electrode materials and the sputtered Pt on ITO-PET. The sputtered Pt on ITO-PET has relatively low transmittance because of the thick, mirror-like Pt layer. b) SEM image of the PEDOT-SWCNT film.

the PE and CE impedance responses appear at much more similar characteristic frequencies (i.e. $\omega = \tau^{-1} = (R_{\mathrm{CE}}C_{\mathrm{d}})^{-1}$, where τ is time constant of the EIS response and C_{d} is the capacitance of the electrochemical double-layer) than those of the other cell types: CE around 100 Hz and the PE between 1-10 Hz (see Fig. 4 b)). This is mainly due to the large C_{d} value of the PEDOT-SWCNT CE (data not shown), which is most likely caused by the large surface area of the porous CE film. For the other CE types, the CE semicircles appear at higher frequencies, and the PE and CE responses are more easily distinguishable. The PE and CE overlapping complicated the EIS equivalent circuit fitting of the PEDOT-SWCNT cells somewhat, resulting in rejection of some of the fit results as unreliable.

All the PEDOT-SWCNT and SWCNT CEs exhibit also an "additional" high frequency arc (between 10 - 100 kHz) in their EIS spectra (Fig. 4 a)), whose value is in the range of 0.1 - 1 Ω, depending on the applied voltage. This may be attributed to a second Nernstian diffusion impedance in the CE pores, as observed previously for porous graphene CEs in the DSC [23].

The series resistance values of all the cell types are very much in the same range, 5-8 $\Omega\mathrm{cm}^2$ (data not shown), as expected based on the similar sheet resistance values of the different CEs.

The R_{CE} values of all the cell types as a function of cell voltage are shown in Fig. 5. The R_{CE} is a measure of the catalytic performance of a counter electrode

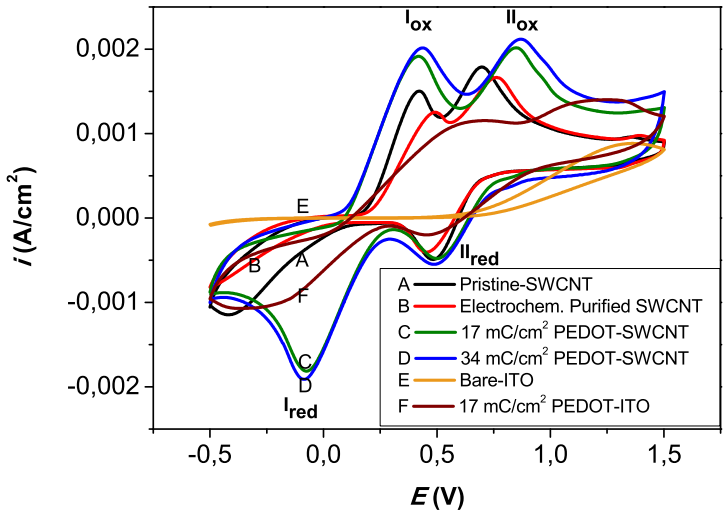

Figure 2: Cyclic voltammograms of the bare SWCNT (as-grown and electrochemically purified), PEDOT-coated SWCNT (deposition charges 17 and 34 mC/cm^2), bare ITO and PEDOT-coated (17 mC/cm^2) ITO electrodes in acetonitrile solutions with 1 mM I_2, 10 mM LiI and 0.1 M $LiClO_4$. Scan rate 0.1 V/s.

and it is inversely proportional to the exchange current density, i_0, of the charge-transfer reaction. The R_{CE} values of the PEDOT-SWCNT CEs are not shown in the voltage range -0.65 – -0.75 V, since in this range the EIS fitting was considered unreliable due to the overlapping of the PE and CE semicircles, as discussed above. In general, the R_{CE} values are lowest for the PEDOT-SWCNT CEs, even lower than for the Pt on FTO glass and ITO-PET CEs, and highest for the SWCNT CEs, indicating that the PEDOT-SWCNT CE is the best CE type in terms of catalytic performance.

Comparison of the R_{CE} as a function of cell current density shows the same relative order between the different type of CEs, with the PEDOT-SWCNT CEs

Table 2: Average photovoltaic parameters of the studied cell types.

CE type	No. of cells	i_{SC} (mA/cm^2)	V_{OC} (V)	F.F. (%)	η (%)
PEDOT-SWCNT	6	11 ± 0.4	0.58 ± 0.01	63 ± 2	4.0 ± 0.1
SWCNT	4	12 ± 0.2	0.61 ± 0.01	28 ± 1	2.0 ± 0.1
sputtered Pt-ITO-PET	4	14 ± 0.5	0.59 ± 0.01	46 ± 2	3.9 ± 0.2
thermal Pt-FTO glass	4	13 ± 0.6	0.59 ± 0.01	58 ± 1	4.3 ± 0.2

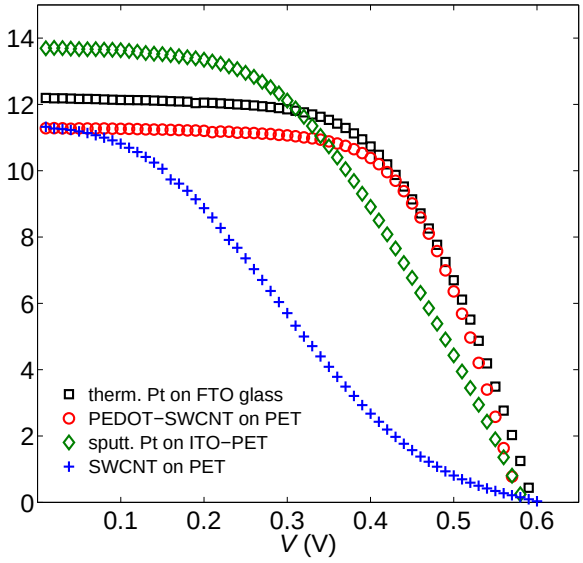

Figure 3: The IV curves of the example DSCs with different counter electrodes: PEDOT-SWCNT film on PET substrate, SWCNT on PET, sputtered platinum on ITO-PET and thermally deposited platinum on FTO glass.

giving clearly the best result (Supporting Information).

The efficiencies of the PEDOT-SWCNT cells were, however, slightly lower than those of the Pt on FTO cells, because of the lower i_{SC} values. The i_{SC} values were also lower for the SWCNT cells. For the SWCNT cells, the i_{SC} is probably at least partially limited by the high R_{CE}, which can be deduced from the shape of the IV curve (no clear plateau near the short-circuit condition). For the PEDOT-SWCNT cells this does not apply, and the reason for the lower i_{SC} must lie elsewhere.

Analysis of the different cell types' PE recombination resistances, R_{REC}, (presented as a whole in the Supporting Information) did not provide an explanation for the SWCNT and PEDOT-SWCNT cells' lower i_{SC}. We measured also the different CE types' reflectances and carried out a theoretical analysis on whether the different reflectance properties could explain the differences in the i_{SC} values, but according to our calculations this was not the case (details in the Supporting Information).

In our previous paper on the SWCNT network CEs [5], we speculated that the lower i_{SC} of the SWCNT-DSCs compared to the reference DSCs could be due to dissolution of residual iron from the SWCNT films (present there from the SWCNT synthesis) into the electrolyte, the iron migrating and depositing to the PE and causing an unwanted effect on the PE performance. To rule out the possibility of such effects in this study, due to dissolution of either

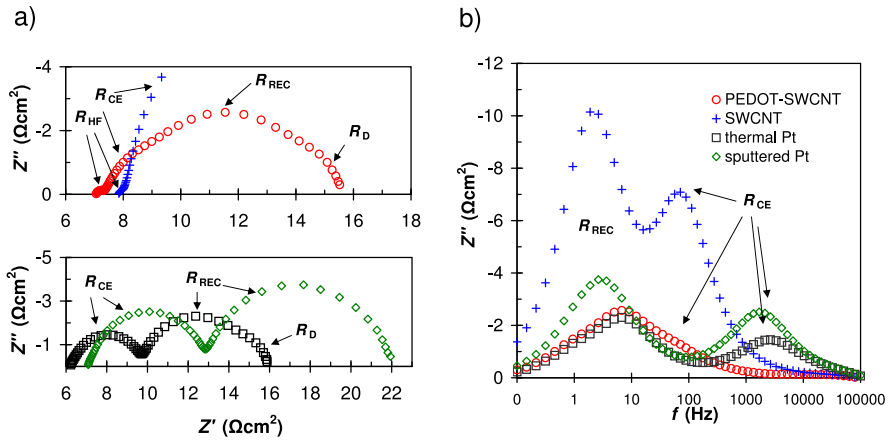

Figure 4: Example EIS spectra of the different cell types, a) Nyquist plot, and b) Bode plot. The DSCs were polarized at -0.8 V. The EIS responces of the different DSC components are marked in the figures, CE = counter electrode, REC = (PE) recombination resistance, HF = high-frequency semicircle of the porous CE, D = diffusion.

iron or PEDOT, the SWCNT and PEDOT-SWCNT electrodes were subjected to extensive cleaning before assembling the DSCs, including e.g. soaking the samples overnight in a large volume of electrolyte solution. Hence, the slightly lower i_{SC} found also here, and unaccounted for by simply optical differences as mentioned above, is surprising. In fact, it appears that the substrates themselves (FTO glass, ITO-PET, PET) may have had an effect on the PE function in these cells, arising from for instance the different chemical composition or water and electrolyte permeability of the substrates and their secondary effects on the PE performance. These observations call for a more closer look on the effect of plastic substrates on the DSC performance, keeping also other possible degradation mechanisms in mind.

4. Conclusions

To replace the platinum catalyst and the transparent conductive indium tin oxide layer of the DSC CE and to obtain flexibility, we fabricated a completely carbon-based counter electrode. Aerosol CVD synthesized SWCNTs were transferred from the filter, to which they were collected from the gas phase, to a PET plastic substrate and electrochemically covered with conductive PEDOT polymer. This allowed us to improve the catalytic activity of the SWCNT network considerably, so that its performance as a DSC CE became comparable to sputtered platinum on an ITO-PET substrate. The PEDOT-SWCNT CE has superior catalytic performance compared to the other CE types studied here

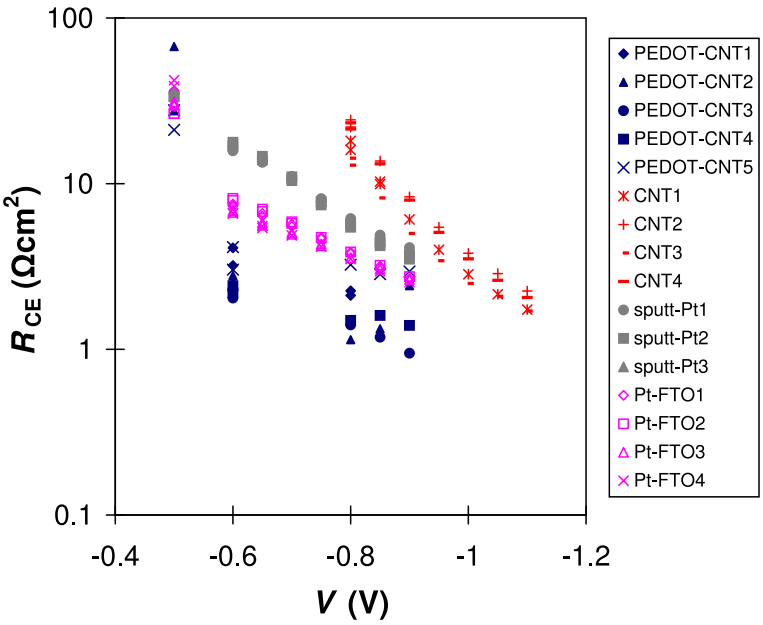

Figure 5: The charge-transfer resistances of the different CE types as a function of cell voltage.

and its sheet resistance meets the requirement of the DSC function at full sun light intensities.

Acknowledgements

This study was carried out in the project MIDE/CNB-E. K. Aitola is grateful for the graduate school of Nordic Center of Excellence in Photovoltaics for the scholarship. V. Ruiz gratefully acknowledges the Academy of Finland (project 125504) and the Spanish Ministry of Science and Innovation (Prog. Ramon y Cajal). A. Nasibulin thanks Academy of Finland (Project Number 128445). We thank Dr. V. Ovchinnikov for carrying out the sputtering.

References

[1] B. O'Regan, M. Grätzel, Nature 353 (1991) 737–740.

[2] L. Ke, R. S. Kumar, S. J. Chua, A. P. Burden, Appl. Phys. A 81 (2005) 969–974.

[3] K. Suzuki, M. Yamaguchi, M. Kumagai, S. Yanagida, Chem. Lett. 8 (2003) 28–29.

[4] J. E. Trancik, S. C. Barton, J. Hone, Nano Lett. 8 (2008) 982–987.

[5] K. Aitola, A. Kaskela, J. Halme, V. Ruiz, A. G. Nasibulin, E. I. Kauppinen, P. D. Lund, J. Electrochem. Soc. 157 (2010) B1831–B1837.

[6] N. Saran, K. Parikh, D.-S. Suh, E. M. noz, H. Kolla, S. K. Manohar, J. Am. Chem. Soc. 126 (2004) 4462–4463.

[7] A. Kaskela, A. G. Nasibulin, M. Y. Timmermans, B. Aitchison, A. Papadimitratos, Y. Tian, Z. Zhu, H. Jiang, D. P. Brown, A. Zakhidov, *et al.*, Nano Lett. 10 (2010) 4349–4355.

[8] Y. Saito, T. Kitamura, Y. Wada, S. Yanagida, Chem. Lett. 31 (2002) 1060–1061.

[9] Y. Saito, W. Kubo, T. Kitamura, Y. Wada, S. Yanagida, J. Photochem. Photobiol. A 164 (2004) 153–157.

[10] Q. Li, J. Wu, Q. Tang, Z. Lan, P. Li, J. Lin, L. Fan, Electrochem. Commun. 10 (2008) 1299–1302.

[11] T. Muto, M. Ikegami, K. Kobayashi, T. Miyasaka, Chem. Lett. 36 (2007) 804–805.

[12] B. Fan, X. Mei, K. Sun, J. Ouyang, Appl. Phys. Lett. 93 (2008) 143103.

[13] K.-M. Lee, W.-H. Chiu, H.-Y. Wei, C.-W. Hu, V. Suryanarayanan, W.-F. Hsieh, K.-C. Ho, Thin Solid Films 518 (2010) 1716–1721.

[14] J. Zhang, X. Li, W. Guo, T. Hreid, J. Hou, H. Su, Z. Yuan, Electrochim. Acta 56 (2011) 3147–3152.

[15] K. Kitamura, S. Shiratori, Nanotechnology 22 (2011) 195703.

[16] W. Hong, Y. Xu, G. Lu, C. Li, G. Shi, Electrochem. Commun. 10 (2008) 1555–1558.

[17] A. Kanciurzewska, E. Dobruchowska, A. Baranhazi, E. Carlegrim, M. Fahlman, M. A. Gîrtu, J. Optoelectron. Adv. Mater. 9 (2007) 1052–1059.

[18] R. Malavé Osuna, V. Hernández, J. T. López Navarrete, E. I. Kauppinen, V. Ruiz, J. Phys. Chem. Lett. 1 (2010) 1367–1371.

[19] A. Moisala, A. G. Nasibulin, D. P. Brown, H. Jiang, L. Khriachtchev, E. I. Kauppinen, Chem. Eng. Sci. 61 (2006) 4393–4402.

[20] A. G. Nasibulin, A. Kaskela, K. Mustonen, A. S. Anisimov, V. Ruiz, S. Kivistö, S. Rackauskas, M. Y. Timmermans, M. Pudas, B. Aitchison, *et al.*, ACS Nano 5 (2011) 3214–3221.

[21] A. Heras, A. Colina, J. López-Palacios, P. Ayala, J. Sainio, V. Ruiz, E. I. Kauppinen, Electrochem. Commun. 11 (2009) 1535–1538.

[22] Z. Huang, X. Liu, K. Li, D. Li, Y. Luo, H. Li, W. Song, L. Chen, Q. Meng, Electrochem. Commun. 9 (2007) 596–598.

[23] J. D. Roy-Mayhew, D. J. Bozym, C. Punckt, I. A. Aksay, ACS Nano 4 (2010) 6203–6211.